RADIO ASTRONOMY

The low density and magnetization of a massive galaxy halo exposed by a fast radio burst

J. Xavier Prochaska[1,2]*, Jean-Pierre Macquart[3], Matthew McQuinn[4], Sunil Simha[1], Ryan M. Shannon[5], Cherie K. Day[5,6], Lachlan Marnoch[6,7], Stuart Ryder[7], Adam Deller[5], Keith W. Bannister[6], Shivani Bhandari[6], Rongmon Bordoloi[8], John Bunton[6], Hyerin Cho[9], Chris Flynn[5], Elizabeth K. Mahony[6], Chris Phillips[6], Hao Qiu[10], Nicolas Tejos[11]

Present-day galaxies are surrounded by cool and enriched halo gas extending for hundreds of kiloparsecs. This halo gas is thought to be the dominant reservoir of material available to fuel future star formation, but direct constraints on its mass and physical properties have been difficult to obtain. We report the detection of a fast radio burst (FRB 181112), localized with arcsecond precision, that passes through the halo of a foreground galaxy. Analysis of the burst shows that the halo gas has low net magnetization and turbulence. Our results imply predominantly diffuse gas in massive galactic halos, even those hosting active supermassive black holes, contrary to some previous results.

The low-density gas located in the outskirts of galaxies influences the process of galaxy formation, especially gas accretion and feedback (*1*). Absorption-line spectroscopy can detect this nearly invisible medium. Surveys demonstrate a very high incidence of cool gas (with temperature $T \sim 10^4$ K), detected through hydrogen Lyman series and continuum absorption, surrounding galaxies with masses similar to that of our Milky Way (*1*, *2*). Properties of this gas depend on galaxy mass but are otherwise insensitive to the galaxy's internal properties (*1*, *3*–*5*). Estimates for the total mass of the cool gas match or exceed the baryonic mass of the galaxy (*4*, *6*). Theoretical treatments of halo gas around present-day galaxies disagree on the proportion of total mass retained in the halo during galaxy formation, with estimates ranging from several tens of percent up to all of the baryons predicted to accrete into the halo (*7*, *8*). This uncertainty stems from observational insensitivity to the hot ($T \gtrsim 10^6$ K) gas that pervades galaxy halos (and within which the cold gas is embedded) and from systematic uncertainties in estimating its mass (*1*, *6*). Constraints on the density and temperature of the halo gas are sufficiently limited to allow qualitatively different descriptions of its ionization and distribution (*9*, *10*). The origin of the cool gas and its composition are challenging to explain theoretically; some models require cosmic rays and magnetic fields to transport material from the central galaxy to sustain the cool medium (*11*).

At coordinated universal time 17:31:15.48365 on 12 November 2018, the Commensal Real-time ASKAP Fast Transients (CRAFT) survey on the Australian Square Kilometer Array Pathfinder (ASKAP) detected a fast radio burst (FRB 181112) from the 12 antennas active at the time. The burst arrival time swept across the observing band (≈1.129 to 1.465 GHz) (Fig. 1A), owing to propagation of the burst through a foreground plasma. The burst sweep yields an estimate of the FRB dispersion measure $\mathrm{DM_{FRB}} = 589.27 \pm 0.03$ pc cm^{-3}, which is the integrated density of electrons n_e at distance r from Earth scaled by $(1+z)^{-1}$, with z the redshift: $\mathrm{DM_{FRB}} \equiv \int n_e/(1+z)\,dr$. The real-time detection triggered full download of the voltage data; these precisely localized the burst to a sky position $21^{\mathrm{h}}49^{\mathrm{m}}23.630^{\mathrm{s}}$, $-52^{\mathrm{d}}58^{\mathrm{m}}15.39^{\mathrm{s}}$ (right ascension, declination, J2000 equinox) with a statistical (systematic) error ellipse oriented at 120° east of north on the sky with major axis $a = 0.555''(3.2'')$ and minor axis $b = 0.153''(0.8'')$ (*12*).

Figure 1B shows a *g*-band image centered on FRB 181112, obtained with the FOcal Reducer/low dispersion Spectrograph 2 (FORS2) instrument on the Very Large Telescope (VLT). It shows the presence of a galaxy coincident with FRB 181112, previously cataloged by the Dark Energy Survey (DES) (*13*) as DES J214923.66–525815.28. The DES and FORS2 data also show a luminous galaxy ≈5″ to the north of the FRB event (DES J214923.89–525810.43). We used follow-up spectroscopy with the FORS2 instrument to measure the redshift (*12*) of the former galaxy as $z = 0.47550$ and that of the latter galaxy as $z = 0.3674$—i.e., in the foreground. We associate FRB 181112 with DES J214923.66–525815.28 (*12*). Compared to the other three known host galaxies of FRBs, the host galaxy of FRB 181112 has an intermediate stellar mass of $M_\star \approx 10^{9.4}$ solar masses ($M_\odot$) (fig. S3) (*12*). It has colors matching star-forming galaxies at $z \sim 0.4$, has an estimated star formation rate of $0.6 M_\odot$ year^{-1}, and shows no signatures of an active galactic nucleus (AGN) (*12*).

The FRB sight line passes at an impact parameter $R_\perp = 29$ kpc from DES J214923.89–525810.43 (hereafter referred to as FG-181112), allowing us to probe the halo of this foreground galaxy. We analyzed the DES, FORS2, and complementary longer-wavelength Wide-field Infrared Survey Explorer (WISE) data to determine FG-181112's physical properties (*12*). We derive a high–stellar mass $\log_{10} M_\star/M_\odot = 10.69^{+0.22}_{-0.46}$, detect nebular emission lines indicative of an AGN and classify it as a Seyfert galaxy, and infer an old (age >1.4 billion years) quiescent stellar population (Table 1 and table S5). Surveys of the halo gas surrounding galaxies of similar mass, with or without AGN activity (*14*), almost ubiquitously reveal strong absorption by cool ($T \sim 10^4$ K) gas for sight lines $R_\perp \leq 100$ kpc. Generally, the inferred total column densities of ionized gas exceed 10^{20} cm^{-2} (*4*, *6*), and transitions of heavy elements indicate a turbulent velocity field (*15*), suggesting that a fraction of the gas has a relatively high density ($n_{\mathrm{H}} \sim 1$ cm^{-3}) (*16*). Such a foreground medium should influence the FRB signal.

The column of gas close to this massive galaxy, however, does not dominate $\mathrm{DM_{FRB}}$. It contributes only $\mathrm{DM_{FG}} \sim 50$ to 120 pc cm^{-3}, depending on assumptions for the density profile and total mass of the halo gas (*12*). The measured $\mathrm{DM_{FRB}}$ is consistent with models that include cosmic gas, our Galaxy, and the host (fig. S9) (*17*, *18*). The sight line to FRB 181112 also intersects the edge of the Fermi Bubbles (*12*), a complex of hot gas encompassing the Galactic Center. The expected DM contribution from gas in these bubbles is small (*12*), but their entrained magnetic field may contribute to the FRB rotation measure (RM).

The RM is the density-weighted integral of the magnetic field parallel to the FRB sight line. The voltages recorded from the ASKAP antennas measure the electric field at the antenna locations in two orthogonal directions on the plane of the sky, enabling the linear polarization fraction of the burst radiation (and its position angle) to be measured as a function of frequency. Averaged over its duration, we find the burst to be ~90% linearly polarized and 10% circularly polarized (*12*). This can be used to estimate the burst RM,

[1]University of California Observatories–Lick Observatory, University of California, Santa Cruz, CA 95064, USA. [2]Kavli Institute for the Physics and Mathematics of the Universe, 5-1-5 Kashiwanoha, Kashiwa, 277-8583, Japan. [3]International Centre for Radio Astronomy Research, Curtin University, Bentley, WA 6102, Australia. [4]Department of Astronomy, University of Washington, Seattle, WA 98195, USA. [5]Centre for Astrophysics and Supercomputing, Swinburne University of Technology, Hawthorn, VIC 3122, Australia. [6]Commonwealth Science and Industrial Research Organisation, Australia Telescope National Facility, P.O. Box 76, Epping, NSW 1710, Australia. [7]Department of Physics and Astronomy, Macquarie University, North Ryde, NSW 2109, Australia. [8]Department of Physics, North Carolina State University, Raleigh, NC 27695, USA. [9]School of Physics and Chemistry, Gwangju Institute of Science and Technology, Gwangju 61005, Korea. [10]Sydney Institute for Astronomy, School of Physics, University of Sydney, Sydney, NSW 2006, Australia. [11]Instituto de Física, Pontificia Universidad Católica de Valparaíso, Casilla 4059, Valparaíso, Chile.
*Corresponding author. Email: xavier@ucolick.org

Downloaded from http://science.sciencemag.org/ on January 16, 2021

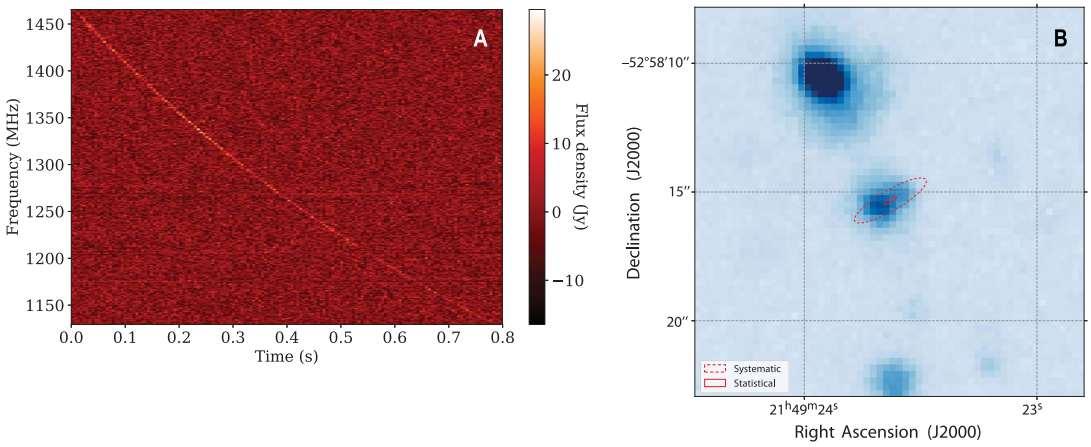

Fig. 1. Dynamic spectrum of FRB 181112 and optical imaging of its host and a coincident foreground galaxy. (**A**) Dynamic spectrum of FRB 181112 recorded by ASKAP. The dispersion measure DM_{FRB} = 589.27 pc cm^{-3}. 1 Jy = 10^{-26} W m^{-2} Hz^{-1}. (**B**) *g*-band FORS2 image centered on FRB 181112, the position of which is depicted by the red ellipses with solid and dashed lines indicating the statistical and systematic uncertainty, respectively. We estimate an additional systematic uncertainty of ≈0.5″ in the astrometric solution of the FORS2 image. The host is well localized to a faint galaxy cataloged as DES J214923.66–525815.28, and one identifies a brighter galaxy (cataloged as DES J214923.89–525810.43, referred to as FG-181112) located ≈5.0″ away at a PA ≈ 13°. The sight line to FRB 181112 passes through the halo of this foreground galaxy at an impact parameter $R_\perp$ = 29 kpc.

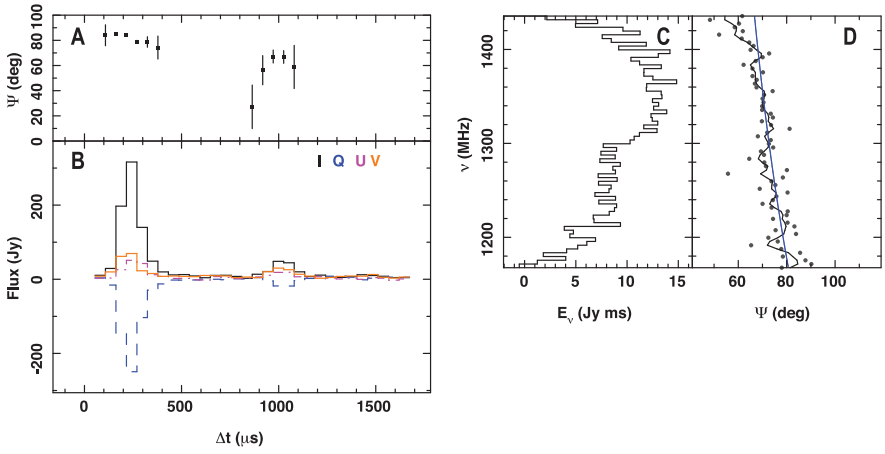

Fig. 2. Spectropolarimetric properties of FRB 181112. (**A**) Relative linear polarization position angle Ψ of the burst averaged in frequency. Error bars indicate uncertainties in the measurements. (**B**) Polarimetric pulse profile of burst in four Stokes components (I, black solid line; Q, blue dashed line; U, purple dashed-dotted line; V, orange solid line). The two pulses, separated by ~800 μs, show different position angles. (**C**) Spectrum of fluence E_ν burst averaged over both pulses. (**D**) Position angle Ψ of the burst plotted as a function of frequency. The gray data points represent measurements in individual frequency channels; the black line denotes these measurements smoothed using a Gaussian kernel with SD = 4 MHz. The variation of the position angle with frequency is the result of Faraday rotation. The blue line shows a maximum likelihood model for polarization, using the inferred RM = 10.9 rad m^{-2}.

as $PA_{obs} = PA_{int} + (c/\nu)^2 RM$, where ν is the frequency, c is the speed of light, and PA_{obs} and PA_{int} are the observed and intrinsic polarization angles, respectively. Figure 2 depicts the frequency sweep of the polarization angle; the apparent ν^{-2} frequency dependence is the RM signature. We fitted an RM model to the sweep, yielding RM = 10.9 ± 0.9 rad m^{-2}. This is a low RM value, consistent (within the uncertainty) with the estimated RM due to our Galaxy toward FRB 181112 (*12*). Adopting an upper limit of RM < 11 rad m^{-2}, we calculate an upper limit for the maximum parallel magnetic field $B_\parallel^{max}$ in the halo of FG-181112: $B_\parallel^{max} < 0.8\ \mu G (n_e/10^{-3}\ cm^{-3})^{-1} (\Delta L/30\ kpc)^{-1}$, in the limit of a perfectly ordered magnetic field with ΔL a characteristic length scale through the halo. We have adopted fiducial values for n_e and L that may characterize the halo of FG-181112 (similar to those adopted for the DM_{FG} estimation). Field reversals would lead us to underestimate $B_\parallel^{max}$. Nevertheless, this low value for $B_\parallel^{max}$ implies that either the magnetic field in the halo is low compared with the interstellar medium or that it is largely disordered.

These constraints have implications for the circumgalactic gas. The magnetic field value in equipartition with the thermal energy of the virialized halo gas is $B_{eq} \equiv \sqrt{8\pi n_e k_B T} = 2\ \mu G (n_e/10^{-3}\ cm^{-3})^{1/2} (T/10^6\ K)^{1/2}$ with k_B the Boltzmann constant. Our $B_\parallel^{max}$ limit is similar to B_{eq} for physically motivated n_e, ΔL, and T, constraining the magnetic field to be near or below equipartition if the total field is similar to the net parallel field. Magnetic fields around the equipartition value enhance the rate of condensation of the hot circumgalactic gas into cooler clouds (*11*), as well as the survival of cool accreting gas (*19*). Near-equipartition field strengths are generated in some models in which cosmic ray pressure transports cool gas and metals to large distances from galaxies (*20*, *21*). Our limit on $B_\parallel^{max}$ is below the mean estimate for sight lines that show strong gas absorption (*22*), despite our sight line likely intersecting gas with similarly strong absorption in FG-181112 (*3*).

The halo gas of FG-181112 broadens the width of the pulse at any given frequency. This temporal broadening τ_{scatt} arises from density fluctuations within the medium, which impose small differences in light-travel time for rays propagating through the gas (*17*, *23*). This scattering is geometrical, and its effects are maximal for a scattering "screen" located at half the distance to the FRB. We determine an upper limit of τ_{scatt} < 40 μs due to scattering, constraining both the turbulent properties of the halo gas and its density. A 3-ms-wide pulse, 150 times the width of the FRB pulse, would still have been detected—i.e., the very narrow width of the FRB 181112 pulse is not the result of observational bias. Figure 2B shows that the temporal profile of FRB 181112 consists of two pulses separated by ~800 μs. The broadening limit is derived by modeling each component as a symmetric intrinsic pulse convolved with the one-sided exponential decay expected as a result of scattering (*12*). Temporal smearing due to inhomogeneities in the plasma distribution along

Downloaded from http://science.sciencemag.org/ on January 16, 2021

the line of sight would otherwise broaden the pulse to a frequency-dependent duration $\tau_{scatt}(\nu) = \tau_0(\nu/1\ \mathrm{GHz})^{\gamma}$, where the index γ is typically ≈ -4 (*12*).

The observed τ_{scatt} constrains the integral of the square of the density along the sight line, $\int dx \delta n_e(x)^2$, which we relate to the electron column density with the parameterization $\langle n_e \rangle \Delta L^{1/2} = \alpha^{-1} (\int dx \delta n_e^2)^{1/2}$, which takes the halo of FG-181112 to have characteristic length ΔL with an average density of $\langle n_e \rangle$. Thus, the parameter α encapsulates the root mean square amplitude of density fluctuations and the volume filling fraction of the turbulence, f_V. The limit on the in situ density assuming a Kolmogorov spectrum of turbulence (*12*) is

$$\langle n_e \rangle < 2 \times 10^{-3} \alpha^{-1} \left(\frac{\Delta L}{50\ \mathrm{kpc}} \right)^{-1/2} \times \left(\frac{L_0}{1\ \mathrm{kpc}} \right)^{1/3} \left(\frac{\tau_{scatt}}{40\ \mu\mathrm{s}} \right)^{5/12} \mathrm{cm}^{-3} \quad (1)$$

where $\Delta L \sim 50$ kpc approximates the path length through the foreground halo and L_0 is the outer scale of turbulence. As the turbulence is likely to be produced by galactic winds and inflows, we expect it to be driven at scales smaller than the impact parameter (~30 kpc) and consider $L_0 = 1$ kpc a reasonable value.

We now examine two standard models for halo gas in which the medium is composed of either hot ($T \sim 10^6$ K) virialized gas or cool gas pressure-confined by the hot gas. In the case of hot virialized gas, our constraint on $\langle n_e \rangle$ suggests densities lower than those expected of ~10^{-3} cm^{-3} gas with kiloparsec driving scales (fig. S12). Because we expect the volume filling factor of this gas to be near unity, the upper limit on the density can be ameliorated only if the gas is much less turbulent (i.e., $\alpha \ll 1$) relative to galactic astrophysical plasmas, especially the interstellar medium of our Galaxy, where $\alpha \sim 7$ (*12*, *24*).

For turbulent, cool 10^4 K clouds embedded in a hot medium, the constraints are stronger. Assuming pressure equilibrium with characteristic values for the hot gas $n_e = 10^{-3}$ cm^{-3} and $T = 2 \times 10^6$ K, application of Eq. 1 with $L_0 = 1$ kpc and $\Delta L = 50$ kpc yields $\alpha < 0.01$. Because $\alpha \propto f_V^{1/2}$, we require a filling factor of cool clouds of $f_V < 10^{-4}$ if the clouds are fully turbulent. Even lower values are required to satisfy this condition if the driving for turbulence within cool clouds is instead at parsec scales, which may be physically motivated (*25*).

These limits on the halo gas density derived from the scattering analysis contradict prior inferences that cool halo gas has a volume filling fraction of $f_V \sim 10^{-3}$ to 10^{-2} (*6*, *26*, *27*). The total neutral hydrogen column density offers the most direct comparison to our result: Photoionization equilibrium constrains the same combination of parameters as scattering, implying

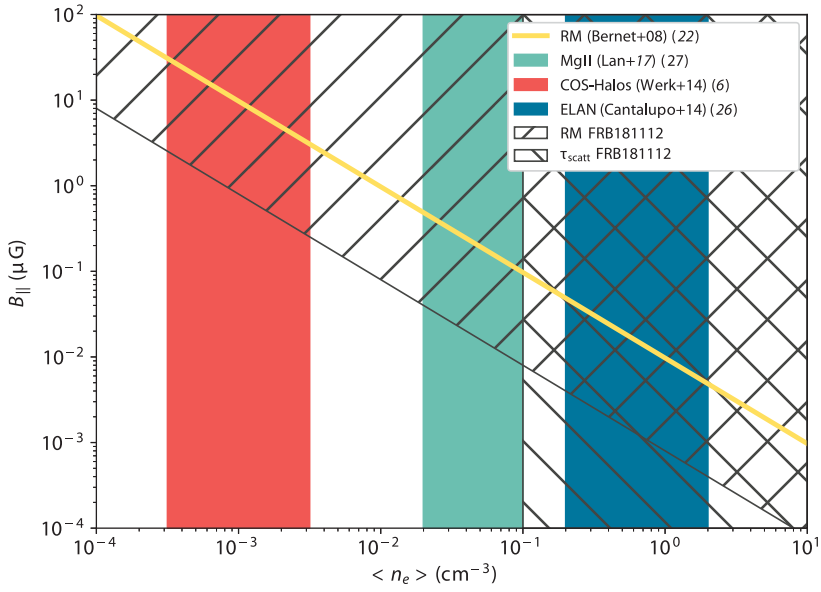

Fig. 3. Constraints on the coherent magnetic field parallel to the line of sight $B_{||}$ and electron density n_e in the halo of FG-181112. The hatched regions show the parameter space in $B_{||}, n_e$ (cool gas) ruled out for the halo of FG-181112 from the measured RM and τ_{scatt} of FRB 181112. These constraints are largely independent of the properties of the foreground galaxy. We compare these results with previous inferences for the density of cool halo gas (colored regions), based on ionization modeling and Lyα fluorescence. We also illustrate previous estimations for the magnetic field strength in halo gas (yellow line) (*22*), which conflict with our results.

Table 1. Properties of FRB 181112, its host, and the foreground galaxy FG-181112. The two uncertainties in right ascension and declination are statistical and systematic, projected onto the coordinate axes. These uncertainties are best described as ellipses with position angle 120° east of north and major and minor axes of $a_{statistical} = 0.55''$, $b_{statistical} = 0.15''$ and $a_{systematic} = 3.2''$, $b_{systematic} = 0.8''$. The coherent magnetic field, density, and filling factor estimates assume a characteristic path length through the halo of $\Delta L = 50$ kpc. The density and filling factor estimates assume a driving scale with root mean density fluctuations of 1 at $L_0 = 1$ kpc, with the bound scaling as $\propto L_0^{1/3}$, as well as a Kolmogorov spectrum of turbulence to separations below the diffractive scale r_{diff}. The filling factor estimate further assumes that cool $T_{cool} = 10^4$ K gas is in pressure equilibrium with hot gas with density $\langle n_e \rangle = 10^{-3}$cm^{-3} and temperature $T_{hot} = 2 \times 10^6$ K hot gas, with the bound scaling as $\propto (\langle n_e \rangle T_{hot}/T_{cool})^{-2}$. See text and (*12*) for details.

Property	Value
FRB	
Right ascension (J2000)	327.34846° ± 0.00007° ± 0.0006°
Declination (J2000)	−52.97093° ± 0.00004° ± 0.0002°
Dispersion measure (DM_{FRB})	589.27 ± 0.03 pc cm^{-3}
Rotation measure (RM)	10.9 ± 0.9 rad m^{-2}
Pulse width	<40 μs
Host galaxy	
Redshift	0.47550 ± 0.00015
Stellar mass	$2.6 \pm 1.1 \times 10^9\ M_\odot$
Star formation rate	0.6 $M_\odot$ year^{-1}
Foreground galaxy FG-181112	
Redshift	0.36738 ± 0.00007
Impact parameter to the FRB sight line ($R_\perp$)	29 ± 3 kpc
Stellar mass	$4.9 \pm 3.2 \times 10^{10}\ M_\odot$
Star formation rate	$<0.3\ M_\odot$ year^{-1}
Coherent magnetic field parallel to the line of sight	$B_{||} < 0.5\ \mu\mathrm{G}(n_e/10^{-3}\ \mathrm{cm}^{-3})$
Density constraint for hot, diffuse gas ($f_V \sim 1$)	$n_e < 2 \times 10^{-3}$ cm^{-3}
Filling factor constraint for cool, clumpy gas	$f_V < 10^{-4}$

Downloaded from http://science.sciencemag.org/ on January 16, 2021

$(n_e/0.1\ \mathrm{cm}^{-3})(f_V/10^{-3})^{1/2}(\Delta L/50\ \mathrm{kpc})^{1/2} \sim 1$ if we take a typical neutral hydrogen column density of 10^{18} cm^{-2} at 30 kpc measured for halos with similar masses as FG-181112 (*4*). Reconciling these values with the scattering from FG-181112 either implies that the cool clouds are less turbulent than assumed or that our sight line has less cool gas than is typical. The foreground galaxy is classified as a Seyfert, with an embedded accreting supermassive black hole in a central AGN that could lead to a more evacuated halo (*28*), although it has been argued that such activity may lead to more cool gas (*29*). Even if the clouds are not turbulent and instead we consider the refractive bending of light through a network of parsec-scale clouds (*25*), we rule out a population of 0.1-pc (or smaller) clouds with $f_V \sim 10^{-3}$ (*12*).

FRBs experience a number of propagation effects that render them sensitive probes of the density, magnetic field, and turbulence of the otherwise elusive gas that pervades galaxy halos. The constraints derived from FRB 181112 for the halo of a massive galaxy are summarized in Fig. 3. The n_e, $B_\parallel$ parameter space ruled out by our observations conflicts with several previous inferences for halo gas (*22*, *26*, *27*). Our observations indicate a density of hot gas that is lower than in many models and also a column of cool gas that is smaller than commonly inferred.

Our results demonstrate that FRBs can be used to elucidate the physical properties of diffuse gas in the halos of galaxies. The multiple pulses observed in FRB 181112 could be due to multipath propagation through the gas. That would be a natural consequence of a medium comprising very low filling factor cool clouds embedded in hot virialized halo gas, with the pulse multiplicity signifying the number of clouds intersected and their arrival times yielding their offsets from the direct burst sight line.

REFERENCES AND NOTES

1. J. Tumlinson, M. S. Peeples, J. K. Werk, *Annu. Rev. Astron. Astrophys.* **55**, 389–432 (2017).
2. J. X. Prochaska, B. Weiner, H.-W. Chen, J. Mulchaey, K. Cooksey, *Astrophys. J.* **740**, 91 (2011).
3. C. Thom *et al.*, *Astrophys. J.* **758**, L41 (2012).
4. J. X. Prochaska *et al.*, *Astrophys. J.* **837**, 169 (2017).
5. R. Bordoloi *et al.*, *Astrophys. J.* **864**, 132 (2018).
6. J. K. Werk *et al.*, *Astrophys. J.* **792**, 8 (2014).
7. Z. Hafen *et al.*, *Mon. Not. R. Astron. Soc.* **488**, 1248–1272 (2019).
8. A. Pillepich *et al.*, *Mon. Not. R. Astron. Soc.* **473**, 4077–4106 (2018).
9. Y. Faerman, A. Sternberg, C. F. McKee, *Astrophys. J.* **835**, 52 (2017).
10. J. Stern *et al.*, *Astrophys. J.* **865**, 91 (2018).
11. S. Ji, S. P. Oh, M. McCourt, *Mon. Not. R. Astron. Soc.* **476**, 852–867 (2018).
12. Materials and methods are available as supplementary materials.
13. T. M. C. Abbott *et al.*, *Astrophys. J.* **239**, 18 (2018).
14. T. A. M. Berg *et al.*, *Mon. Not. R. Astron. Soc.* **478**, 3890–3934 (2018).
15. H.-W. Chen *et al.*, *Astrophys. J.* **724**, L176–L182 (2010).
16. T.-W. Lan, H. Mo, *Mon. Not. R. Astron. Soc.* **486**, 608–622 (2019).
17. M. McQuinn, *Astrophys. J.* **780**, L33 (2014).
18. J. X. Prochaska, Y. Zheng, *Mon. Not. R. Astron. Soc.* **485**, 648–665 (2019).
19. T. Berlok, C. Pfrommer, *Mon. Not. R. Astron. Soc.* **485**, 908–923 (2019).
20. R. Pakmor, C. Pfrommer, C. M. Simpson, V. Springel, *Astrophys. J.* **824**, L30 (2016).
21. I. S. Butsky, T. R. Quinn, *Astrophys. J.* **868**, 108 (2018).
22. M. L. Bernet, F. Miniati, S. J. Lilly, P. P. Kronberg, M. Dessauges-Zavadsky, *Nature* **454**, 302–304 (2008).
23. J.-P. Macquart, J. Y. Koay, *Astrophys. J.* **776**, 125 (2013).
24. K. R. Anantharamaiah, R. Narayan, in *Radio Wave Scattering in the Interstellar Medium*, J. M. Cordes, B. J. Rickett, D. C. Backer, Eds., vol. 174 of *American Institute of Physics Conference Series* (AIP, 1988), pp. 185–189.
25. M. McCourt, S. P. Oh, R. O'Leary, A.-M. Madigan, *Mon. Not. R. Astron. Soc.* **473**, 5407–5431 (2018).
26. S. Cantalupo, F. Arrigoni-Battaia, J. X. Prochaska, J. F. Hennawi, P. Madau, *Nature* **506**, 63–66 (2014).
27. T.-W. Lan, M. Fukugita, *Astrophys. J.* **850**, 156 (2017).
28. E. Choi, J. P. Ostriker, T. Naab, L. Oser, B. P. Moster, *Mon. Not. R. Astron. Soc.* **449**, 4105–4116 (2015).
29. L. P. David *et al.*, *Astrophys. J.* **792**, 94 (2014).
30. R. Shannon, S. Bhandari, C. Day, E. Mahony, A. Deller, C. Phillips, FRB 181112 ATCA observations, v1, CSIRO Data Collection (2019); https://doi.org/10.25919/5d7e19c34743c.
31. J. X. Prochaska *et al.*, FRBs/FRB: First DOI release of this repository, Version v1.0.0, Zenodo (2019); doi: https://doi.org/10.5281/zenodo.3403651.

ACKNOWLEDGMENTS

We are grateful to the Australia Telescope National Facility (ATNF) operations staff and the Murchison Radio-astronomy Observatory staff for supporting our ASKAP operations and to the ATNF Director and Steering Committee for dedicating time for these observations. Work at the Naval Research Laboratory is supported by NASA. The Australian Square Kilometre Array Pathfinder, Australia Telescope Compact Array, and Parkes Radio Telescope are part of the Australia Telescope National Facility, which is managed by CSIRO. Operation of ASKAP is funded by the Australian government, with support from the National Collaborative Research Infrastructure Strategy. ASKAP uses the resources of the Pawsey Supercomputing Centre. ASKAP, the Murchison Radio-astronomy Observatory, and the Pawsey Supercomputing Centre are initiatives of the Australian Government, with support from the government of Western Australia and the Science and Industry Endowment Fund. We acknowledge the Wajarri Yamatji as the traditional owners of the Murchison Radio-astronomy Observatory site. **Funding:** J.X.P. and S.S. are supported by the National Science Foundation grant AST-1911140. K.W.B., J.-P.M, and R.M.S. acknowledge Australian Research Council (ARC) grant DP180100857. A.T.D. is the recipient of an ARC Future Fellowship (FT150100415). R.M.S. acknowledges support through ARC grants FL150100148 and CE170100004. N.T. acknowledges support from PUCV research funding 039.333/2018. **Author contributions:** J.X.P., J.-P.M., M.M., S.S., R.M.S, C.F., and C.K.D. drafted the manuscript. J.X.P., N.T., S.R., L.M, S.S., and E.K.M. obtained, reduced, and interpreted optical observations. R.B. performed the Fermi Bubble analysis. K.W.B. built the search and voltage capture software. A.D., C.P., C.K.D. H.C., H.Q., and S.B., designed, built, and conducted the correlation, calibration, and imaging software to localize FRB 181112. R.M.S. led the ASKAP observing and interpreted radio band polarization data. E.K.M. and S.B. obtained, reduced, and interpreted ATCA data. J.B. designed the ASKAP digital systems. **Competing interests:** The authors declare no competing interests. **Data and materials availability:** This work is based on observations collected at the European Southern Observatory, available from http://archive.eso.org/ under program ID 0102.A-0450(A) (PI: Macquart); before the ESO proprietary period expires, they can be obtained at https://drive.google.com/drive/folders/15QrdfZqJbNAnj-mGdOHX9t8nSBLcf9sZ. Observations from the Australia Telescope Compact Array are available at the CSIRO Data Access Portal (*30*). Additional datasets used in this paper are available from the gSTAR Data Management and Collaboration Platform (gDMCP) at https://data-portal.hpc.swin.edu.au/dataset/askap-visibilities-and-images-for-frb181112, including the nine ASKAP visibility datasets used to calibrate and determine the localization of FRB 181112, radio images of the FRB and surrounding field, and the ATCA images used for astrometric alignment. Reduced data and scripts are available at Zenodo (*31*). Data reduction scripts and code written by the coauthors for this project are available from the CRAFT git repository https://bitbucket.csiro.au/scm/craf/craft.git, the PSRVLBIREDUCE repository https://github.com/dingswin/psrvlbireduce, the FRB repository https://github.com/FRBs/FRB, and the PYPEIT repository https://github.com/pypeit/pypeit.

SUPPLEMENTARY MATERIALS

science.sciencemag.org/content/366/6462/231/suppl/DC1
Materials and Methods
Supplementary Text
Figs. S1 to S12
Tables S1 to S7
References (*32*–*86*)

20 May 2019; accepted 17 September 2019
Published online 26 September 2019
10.1126/science.aay0073

Downloaded from http://science.sciencemag.org/ on January 16, 2021

Science

The low density and magnetization of a massive galaxy halo exposed by a fast radio burst

J. Xavier Prochaska, Jean-Pierre Macquart, Matthew McQuinn, Sunil Simha, Ryan M. Shannon, Cherie K. Day, Lachlan Marnoch, Stuart Ryder, Adam Deller, Keith W. Bannister, Shivani Bhandari, Rongmon Bordoloi, John Bunton, Hyerin Cho, Chris Flynn, Elizabeth K. Mahony, Chris Phillips, Hao Qiu and Nicolas Tejos

Science **366** (6462), 231-234.
DOI: 10.1126/science.aay0073originally published online September 26, 2019

Probing a galaxy halo with a radio burst

Fast radio bursts (FRBs) are millisecond flashes of radio emission from distant galaxies. It has only recently become possible to locate single bursts precisely enough to determine the host galaxy. Prochaska *et al.* have observed and localized a FRB using a radio interferometer. The line of sight to the host galaxy coincidentally passes through the outskirts of a closer foreground galaxy. By analyzing the propagation of the FRB, the authors put constraints on the density and magnetization of gas in the outskirts of the foreground galaxy. The technique provides complementary information to existing methods using background quasars.

Science, this issue p. 231

ARTICLE TOOLS http://science.sciencemag.org/content/366/6462/231

SUPPLEMENTARY MATERIALS http://science.sciencemag.org/content/suppl/2019/09/25/science.aay0073.DC1

REFERENCES This article cites 82 articles, 1 of which you can access for free
http://science.sciencemag.org/content/366/6462/231#BIBL

PERMISSIONS http://www.sciencemag.org/help/reprints-and-permissions

Use of this article is subject to the Terms of Service

Science (print ISSN 0036-8075; online ISSN 1095-9203) is published by the American Association for the Advancement of Science, 1200 New York Avenue NW, Washington, DC 20005. The title *Science* is a registered trademark of AAAS.

Copyright © 2019 The Authors, some rights reserved; exclusive licensee American Association for the Advancement of Science. No claim to original U.S. Government Works

Downloaded from http://science.sciencemag.org/ on January 16, 2021